

Seismic characterization of an active metamorphic massif, Nanga Parbat, Pakistan Himalaya

Anne Meltzer
Golam Sarker*
Bruce Beaudoin*
Leonardo Seeber
John Armbruster

Earth and Environmental Sciences, Lehigh University, Bethlehem, Pennsylvania 18015, USA

Lamont-Doherty Earth Observatory, Palisades, New York 10964, USA

ABSTRACT

Earthquakes recorded by a dense seismic array at Nanga Parbat, Pakistan, provide new insight into synorogenic metamorphism and mass flow during mountain building. Microseismicity beneath the massif drops off sharply with depth and defines a shallow transition between brittle failure and ductile flow. The base of seismicity bows upward, mapping a thermal boundary with 3 km of structural relief over a lateral distance of 12 km. Anomalous low seismic velocities are observed at the core of the massif and extend to depth through the crust. The main locus of seismicity and low velocities correlates with a region of high topography, rapid exhumation, high geothermal gradients, young metamorphic and igneous ages, and crustal fluid flow. We suggest a genetic link between these phenomena in which hot rocks, rapidly advected from depth, are pervasively modified at relatively shallow levels in the crust.

INTRODUCTION

Nanga Parbat is at the western end of the Himalaya in the western syntaxis. Its 8126 m summit and the Indus River at its base define the world's largest relief (7 km vertical in 21 km horizontal). The Indian plate rocks of Nanga Parbat, part of the Nanga Parbat–Haramosh massif, are polymetamorphic. Their Precambrian protolith was overprinted by Tertiary continental collision between India and Asia (Wheeler et al., 1995), and recent pervasive modification of the crust is documented by young (3 Ma) migmatites, the result of in situ melting of host rock under low-pressure (4–6 kbar), high-temperature (600–700 °C) metamorphic conditions (Poage et al., 2000; Whittington et al., 1999; Zeitler et al., 1993). Young (1–2 Ma) granitic plutons and dikes record recent anatexis linked to isothermal decompression (Zeitler et al., 1993). U–Pb, Ar–Ar, and fission-track ages document rapid cooling, and with petrologic evidence and fluid-inclusion data, document rapid exhumation at rates as high as 5–10 mm/yr over the past 3 m.y. (Schneider et al., 1999; Treloar et al., 1989; Winslow et al., 1994, 1996; Zeitler, 1985). Locally the Raikhot fault, an active thrust, overprints and even faults away the original collisional suture, the Main Mantle thrust (Butler and Prior, 1988). The Raikhot fault juxtaposes Nanga Parbat gneiss against mafic rocks of the Kohistan island arc and in places thrusts crystalline basement over Quaternary gravels (Shroder et al., 1989). Boiling

hot springs occur within the massif, and hydrothermal alteration is observed in numerous outcrops. All these observations suggest a level of vigorous tectonic activity distinct from surrounding terranes and a potentially anomalous thermal structure beneath the massif. As part of a multidisciplinary study to understand the active processes responsible for crustal reworking at Nanga Parbat, we deployed a dense seismic array to characterize seismicity and determine crustal structure beneath the massif.

NANGA PARBAT SEISMIC EXPERIMENT

A number of studies have improved our understanding of subsurface structure in mountain belts at regional scales, but detailed characterizations of crustal structure and igneous and metamorphic processes in active orogens is lacking. The high and rugged topography associated with these settings makes dense regional deployments of seismic arrays difficult. Our array at Nanga Parbat consisted of 6 broadband and 50 short-period three-component seismometers (Fig. 1). Stations were deployed along the Indus and Astor river valleys, and along glacial valleys in the interior of the massif. Four additional broadband stations were deployed in a more regional context, enlarging the total aperture of the network to ~300 km to provide better constraints for locating regional events. In a 4 month time window, we recorded more than 1500 events comprising teleseismic, regional, and local earthquakes (Fig. 1). Primary source regions are the Pamir–Hindu Kush, the Karakoram, the Himalayan and Hazara arcs, and local seismicity beneath the massif. Abundant seismic-

ity associated with the Pamir–Hindu Kush region originates 200–300 km northwest of Nanga Parbat at 100–300 km depth and serves as a beam source to illuminate structure beneath the massif.

RESULTS

Microseismicity at Nanga Parbat is distributed along strike beneath the massif, but exhibits a sharp drop-off to its west and a more gentle drop-off east of the main summit ridge (Fig. 1). The adjacent Kohistan terrane is virtually aseismic. The sharp cutoff in seismicity to the west corresponds to the mapped trace of the Raikhot fault where it is coincident with the Indus River. Brittle deformation is largely restricted to depths ≤ 2 km below sea level (bsl), ~5–6 km below the average topographic surface; 92% of the local events occurred within this depth range. The base of seismicity forms a prominent antiformal shape beneath the massif and exhibits considerable structural relief, ~3 km in a lateral distance of 12 km (Fig. 2). The apex of this antiform occurs at 5 km depth bsl and is offset ~10 km northwest of the topographic ridge crest. The base of seismicity deepens to 8 km bsl to the northwest and southeast, mapping a thermal boundary and a transition between brittle and plastic deformation that takes place over an ~3-km-thick zone. There is no seismicity deeper than 8 km depth bsl beneath the massif.

The transition from brittle to plastic deformation in Earth occurs over a range of temperatures depending on rock composition, fluid content, pressure, and strain rate. At Nanga Parbat high-grade granitic gneiss and quartzofeldspathic biotite gneiss dominate. For dry quartzofeldspathic rocks, the brittle to ductile transition occurs between 300 and 450 °C (Fournier, 1991; Scholz, 1988). Fluid inclusions in veins suggest that at Nanga Parbat this transition occurs at the upper end of this range: primary fluid inclusions from veins associated with brittle fractures that cut young structures include a vapor-rich phase that homogenized at temperatures to 415 °C, whereas fluid inclusions from ductilely deformed veins are inferred to have equilibrated at 450 °C (Craw et al., 1994, 1997). High thermal gradients of ~60 °C/km in the shallow crust are also indicated by petrologic and thermochronologic data

*Present addresses: Sarker—Texas A&M, 1000 Discovery Road, College Station, Texas 77843, USA; Beaudoin—IRIS PASSCAL, New Mexico Tech, Socorro, New Mexico 87801, USA.

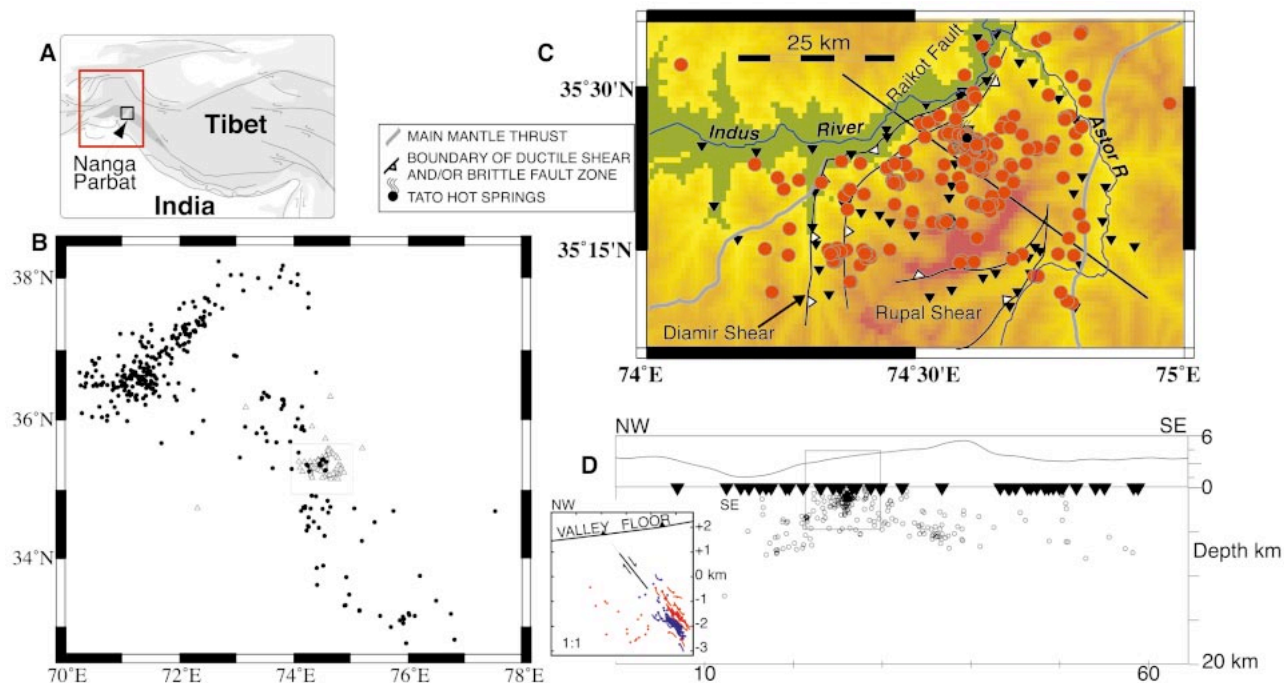


Figure 1. A: Regional location map; area in red box is shown in B. B: Seismic array (triangles) and regional and local events (circles) recorded. Area outlined by box is detailed in C. C: Station locations (triangles) and local events (red circles). Base is topography. D: Epicenters in C projected to cross section. Line of section is shown in C. Inset shows relocation of events in box using cross-correlation technique (arrival time locations in red, cross-correlation locations in blue).

(Poage et al., 2000; Winslow et al., 1994). Along such high thermal gradients, rocks pass through the 400–450 °C isotherm at shallow depths, below which they enter the ductile regime. The high temperatures associated with the brittle-plastic transition imply that there is little fluid interaction with the rock matrix within this zone; as little as 0.2% water produces pronounced hydrolytic weakening, lowering the temperature at which plastic deformation takes place. This result seems counterintuitive given that an active hydrothermal system, including boiling hot springs, is observed at the surface, but is consistent with the high resistivities (1000 ohm-m) determined by magnetotelluric measurements at Nanga Parbat, which imply that the crust beneath the massif has little aqueous fluid (Park and Mackie, 2000). This result is also consistent with the relatively unique hydrothermal system at Nanga Parbat, in which boiling fluids dominate to ~2 km depth bsl and an unusual dry-steam system (vapor phase only) dominates below these depths (Craw et al., 1994, 1997).

Most of the local seismic events recorded by our array have clean impulsive signals, allowing high-quality focal mechanisms to be determined. Although we recorded some thrust and some right-lateral strike-slip focal mechanisms, much of the observed seismicity exhibits mechanisms consistent with extension above the doubly vergent thrust system bounding the massif. Neither structural mapping nor seismicity show evidence for low-angle crustal-scale normal faults typically as-

sociated with tectonic denudation in orogenic belts (Edwards et al., 2000; Schneider et al., 1999). A cluster of seismicity associated with the Tato hot springs included a swarm of 26 events in a 24 h period. When relocated using cross-correlation techniques, hypocenters locate within ± 50 m of each other and define a fault plane that may serve as a pathway for circulation of meteoric water to and from the surface (Fig. 1, inset).

Prominent but complicated S wave arrivals at stations throughout the array rule out the possibility of a substantial magma body beneath Nanga Parbat, which had been a possible explanation for many of the igneous, metamorphic, and structural observations. This observation holds for both Hindu Kush events with a relatively vertical ray path beneath the massif such that they sample the entire crust and local events traveling more obliquely through the shallow crust. A three-dimensional joint inversion for hypocenter location, V_p , and V_s (Roecker et al., 1993) shows that the seismic velocity structure beneath the Nanga Parbat massif is anomalously low; velocities are reduced as much as 10% over lateral distances of 10–20 km (Fig. 2; Table 1). In the inversions, the target region is parameterized as a set of uniform 10 km by 10 km blocks. The parameterization allows both vertical and lateral variations in velocity, and P and S wave velocities are solved as independent parameters. The data set for this inversion comprises 8534 P and 6486 S arrivals from 365 high-quality regional and local events and 239

teleseisms. Both P and S wave low-velocity anomalies are observed within the core of the massif and extend to depth through the entire crust. The uppermost-mantle velocity, determined from teleseismic P arrivals, is also ~10% slower within the core of the massif ($V_p = 7.5$ km/s) compared to the surrounding mantle velocity ($V_p = 8.2$ km/s). The depth to the Moho, as determined from best-fit one-dimensional velocity-model inversions and preliminary receiver-function analysis, is 40 km. A crustal thickness of 40 km, while thin by Himalayan standards, is consistent with the few regional observations of crustal thickness in the region (Mooney et al., 1998).

We interpret the low-velocity anomalies to represent elevated temperatures at depth. The distribution of low-velocities and confining pressure at depth, along with magnetotelluric and petrologic data, rule out the possibility of significant fracture porosity or elevated pore pressure as an explanation. In addition, significant attenuation of both P and S waves is observed in waves traveling through the massif compared to those that do not (Sarker et al., 1999). The base of seismicity and distri-

TABLE 1. P (V_p) AND S (V_s) WAVE VELOCITIES AT NANGA PARBAT

Depth Range	Velocity—Massif Core		Velocity—Surrounding Area	
	V_p km/s	V_s km/s	V_p km/s	V_s km/s
<7 km depth	5.5–5.8	3.2–3.5	5.9–6.2	3.5–3.7
7–20 km	5.6–5.75	3.4–3.5	6.3–6.5	3.6–3.8
20–40 km	5.6–6.0	3.4–3.7	6.4–6.6	3.7–3.9

bution of low velocities found at Nanga Parbat is consistent with the prediction of thermal models that show that rapid advection will steepen the geotherm and that Nanga Parbat should resemble a column of hot rock rising toward the surface (Craw et al., 1994). The focused low-velocity anomaly extends through the entire crust and suggests that the primary flow path of material into the massif is from depth rather than along a shallow detachment. Our seismic results indicate that the dramatically high topography of Nanga Parbat is above thin, hot, weak, crust.

Estimates of thermal gradients from thermobarometry suggest that temperatures at depths of 14–20 km beneath Nanga Parbat reach 600–800 °C (Poage et al., 2000; Whittington et al., 1999). The 5%–10% reduction in seismic velocity observed in the core of the massif is consistent with temperatures in this range (Christensen and Mooney, 1995). At these temperatures, felsic rocks are hot enough to partially melt. Although there is no evidence of a large continuous magma body beneath Nanga Parbat, we see local traveltime delays and anomalous waveforms suggesting small-scale heterogeneity possibly related to small partial-melt zones consistent with migmatization. Local events display a large variation in waveform coda associated with propagation path (Fig. 3).

DISCUSSION

The main locus of seismicity and the regions of low seismic velocity correlate with the area of most rapid exhumation, cooling ages younger than 2 Ma, young granitic dikes and plutons, young migmatites formed under low-pressure, high-temperature conditions, and high crustal resistivity (Zeitler et al., 2001). These observations are all restricted to the core of the massif. The central part of the massif is bounded by two primary shear zones, the Raikhot-Diamir and Rupal, across which major discontinuities in cooling ages, metamorphic facies, and the age of igneous and metamorphic activity are observed (Poage et al., 2000; Schneider et al., 1999). Zeitler et al. (2001) proposed a thermal-mechanical-erosional model coupling exhumation, accentuated by river incision, to metamorphism and melting in the crust. The distribution of seismicity and low seismic velocities is consistent with this model in which rapid exhumation leads to pervasive modification of continental crust as hot rocks flow rapidly from depth to the surface. As this material is brought to the surface, advection of isotherms results in low P and S wave velocities throughout the crust and elevates the position of the brittle-ductile transition, causing it to bow convex upward beneath the massif. Brittle fracturing predominates above 2 km depth (bsl). In this region, meteoric water circulates

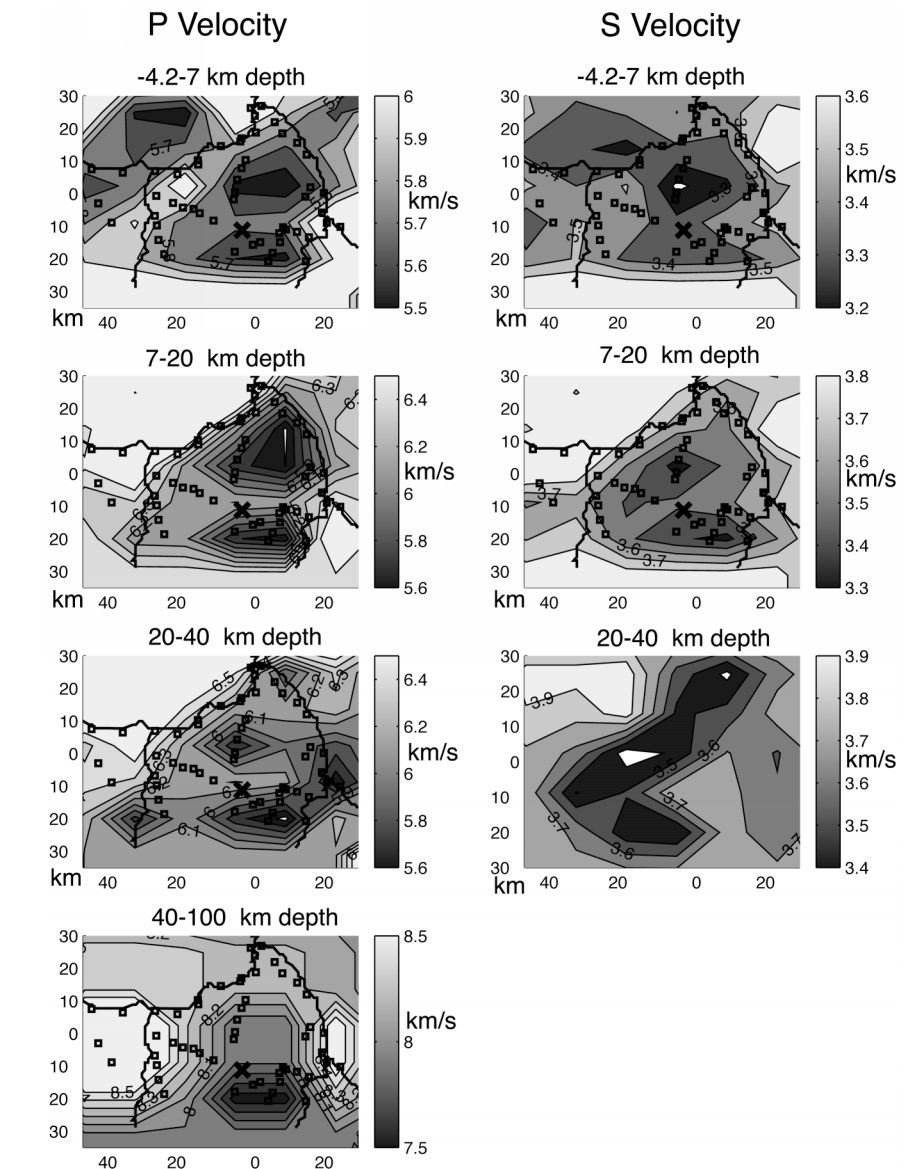


Figure 2. Depth slices through three-dimensional joint inversion for hypocenter location, V_p , and V_s . Both P and S wave low-velocity anomalies are centered at core of massif and extend to depth throughout entire crust. Depth slices are in kilometers below sea level (negative numbers = positive elevation). Darker shading indicates lower seismic velocity. Map area is same as outlined in Figure 1C. Squares indicate stations. X indicates Nanga Parbat summit.

and an active hydrothermal system exists. The transition from brittle to plastic deformation takes place within a 3-km-thick zone beneath this region. Equating the base of seismicity to the 450 °C isotherm yields a geothermal gradient of 56 °C/km. At depths of 14–20 km beneath the massif, temperatures reach 600–800 °C and decompression melts are generated. As continental crust passes through this region, it is pervasively modified. The result is a sharply focused metamorphic anomaly separated in time and space from the main collisional event. The base of seismicity maps out an antiform beneath the massif. The apex of the antiform is offset from the topographic ridge crest reflecting the flow of material from depth and is consistent with particle paths developed in a two-

sided orogen (Koons, 1990). This leads to the final conclusion that the remarkably high topography at Nanga Parbat is above hot, thin, weak crust, dynamically supported by the continuous flow of material from depth.

ACKNOWLEDGMENTS

This research is supported by the Continental Dynamics Program, Earth Sciences Division, National Science Foundation (grant EAR-9418849), and the Incorporated Research Institutes in Seismology. We thank members of the Nanga Parbat Working Group: Page Chamberlain, Dave Craw, Bill Kidd, Peter Koons, Steve Park, and Peter Zeitler for discussions and insight.

REFERENCES CITED

Butler, R.W.H., and Prior, D.J., 1988, Tectonic controls on the uplift of the Nanga Parbat massif, Pakistan Himalayas: *Nature*, v. 333, p. 247–250.

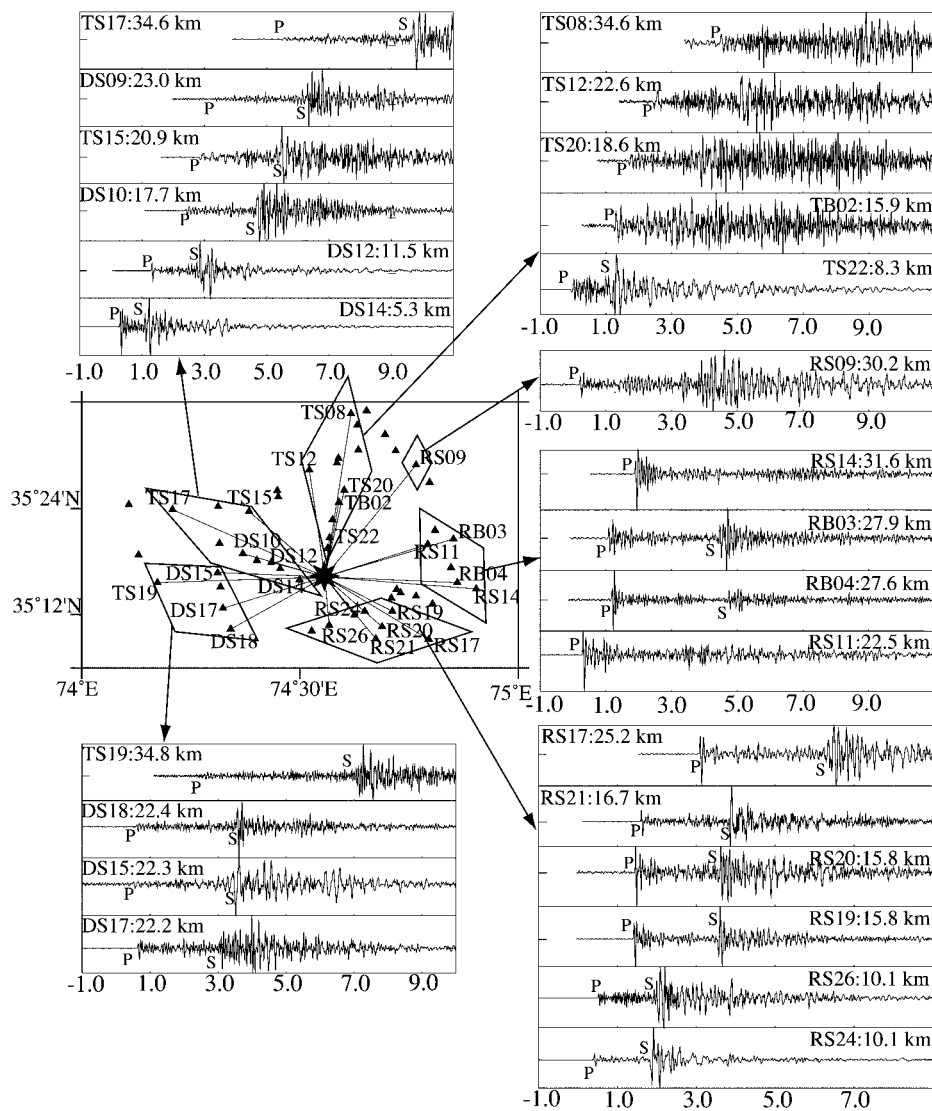


Figure 3. True amplitude reduced record sections for local event plotted according to azimuth and distance. Reduction velocity is 6.0 km/s. Polygons outline stations plotted in each section. Star indicates epicenter, triangles are stations. Station names and distances from event are indicated. See Figure 1 for location of array. Note variation in character of arrivals across array. Many stations show clear P and S phases, but others do not. In particular note appearance of arrivals at Tato stations north of event. In contrast, arrivals at these stations from other local events (following different ray paths) show clear and impulsive P and S phases. Also note attenuation of S phase at several stations located east of event (RS14 and RS11).

Christensen, N.I., and Mooney, W.D., 1995, Seismic velocity structure and composition of the continental crust: A global view: *Journal of Geophysical Research*, v. 100, p. 9761–9788.

Craw, D., Koons, P.O., Winslow, D., Chamberlain, C.P., and Zeitler, P.K., 1994, Boiling fluids in a region of rapid uplift, Nanga Parbat massif, Pakistan: *Earth and Planetary Science Letters*, v. 128, p. 169–182.

Craw, D., Chamberlain, C.P., Zeitler, P.K., and Koons, P.O., 1997, Geochemistry of a dry steam geothermal zone formed during rapid uplift of Nanga Parbat, northern Pakistan: *Chemical Geology*, v. 142, p. 11–22.

Edwards, M.A., Kidd, W.S.F., Khan, M.A., and Schneider, D.A., 2000, Tectonics of the SW margin of Nanga Parbat–Haramosh Massif, in Khan, M.A., et al., eds., *Tectonics of the Nanga Parbat syntaxis and the western Himalaya:*

Geological Society [London] Special Publication 170, p. 77–100.

Fournier, R.O., 1991, The transition from hydrostatic to greater than hydrostatic fluid pressure in presently active continental hydrothermal systems in crystalline rock: *Geophysical Research Letters*, v. 18, p. 955–958.

Koons, P.O., 1990, The two-sided wedge in orogeny: Erosion and collision from the sand box to the Southern Alps, New Zealand: *Geology*, v. 18, p. 679–682.

Mooney, W.D., Laske, G., and Masters, T.G., 1998, CRUST 5.1: A global crustal model at 5° × 5°: *Journal of Geophysical Research*, v. 103, p. 727–747.

Park, S.K., and Mackie, R.L., 2000, Resistive (dry?) lower crust in an active orogen, Nanga Parbat, northern Pakistan: *Tectonophysics*, v. 316, p. 359–380.

Poage, M.A., Chamberlain, C.P., and Craw, D., 2000, Massif-wide metamorphism and fluid evolution at Nanga Parbat, northwestern Pakistan: *American Journal of Science*, v. 300, p. 463–482.

Roecker, S.W., Sabitova, T.M., Vinnik, L.P., Burmakov, Y.A., Golvanov, M.I., Mamatkanova, R., and Munirova, L., 1993, Three-dimensional elastic wave velocity structure of the western and central Tien Shan: *Journal of Geophysical Research*, v. 98, p. 15 779–15 795.

Sarker, G.L., Meltzer, A.S., Seiber, L., and Armbruster, J., 1999, Seismic attenuation and evidence of thermal anomalies beneath Nanga Parbat, western Himalaya [abs.]: *Eos (Transactions, American Geophysical Union)*, v. 80, p. F722.

Schneider, D.A., Edwards, M.A., Kidd, W.S.F., Khan, M.A., Seiber, L., and Zeitler, P.K., 1999, Tectonics of Nanga Parbat, western Himalaya: Synkinematic plutonism within the doubly vergent shear zones of a crustal-scale pop-up structure: *Geology*, v. 27, p. 999–1002.

Scholz, C.H., 1988, The brittle-plastic transition and the depth of seismic faulting: *Geologische Rundschau*, v. 77, p. 319–328.

Shroder, J.F., Khan, M.S., Lawrence, R.D., Madin, I.P., and Higgins, S., 1989, Quaternary glacial chronology and neotectonics in the Himalaya of northern Pakistan, in Malinconico, L.L., and Lillie, R.J., eds., *Tectonics of the western Himalayas: Geological Society of America Special Paper* 232, p. 275–294.

Treloar, P.J., Rex, D.C., Guise, P.G., Coward, M.P., Searle, M.P., Windley, B.F., Petterson, M.G., Jan, M.Q., and Luff, I.W., 1989, K-Ar and Ar-Ar geochronology of the Himalayan collision in NW Pakistan: Constraints on the timing of suturing, deformation, metamorphism, and uplift: *Tectonics*, v. 8, p. 881–909.

Wheeler, J., Treloar, P.J., and Potts, G.J., 1995, Structural and metamorphic evolution of the Nanga Parbat syntaxis, Pakistan Himalaya, on the Indus gorge transect: The importance of early events: *Geological Journal*, v. 30, p. 349–371.

Whittington, A.G., Harris, N., and Butler, R.W.H., 1999, Contrasting anatexis styles at Nanga Parbat, northern Pakistan, in Macfarlane, A., et al., eds., *Himalaya and Tibet: Mountain roots to mountain tops: Geological Society of America Special Paper* 328, p. 129–144.

Winslow, D.M., Zeitler, P.K., and Chamberlain, C.P., 1994, Direct evidence for steep geotherm under conditions of rapid denudation, western Himalaya, Pakistan: *Geology*, v. 22, p. 1075–1078.

Winslow, D., Zeitler, P.K., Chamberlain, C.P., and Williams, I.S., 1996, Geochronologic constraints on syntaxial development in the Nanga Parbat region, Pakistan: *Tectonics*, v. 15, p. 1292–1308.

Zeitler, P.K., 1985, Cooling history of the northwestern Himalaya, Pakistan: *Tectonics*, v. 4, p. 127–151.

Zeitler, P.K., Chamberlain, C.P., and Smith, H.A., 1993, Synchronous anatexis, metamorphism, and rapid denudation at Nanga Parbat (Pakistan Himalaya): *Geology*, v. 21, p. 347–350.

Zeitler, P.K., Meltzer, A.S., Koons, P.O., Craw, D., Hallet, B., Chamberlain, C.P., Kidd, W.S.F., Park, S., Seiber, L., Bishop, M., and Shroder, J., 2001, Erosion, Himalayan geodynamics, and the geology of metamorphism: *GSA Today*, v. 11, no.1, p. 4–9.

Manuscript received August 28, 2000

Revised manuscript received March 2, 2001

Manuscript accepted March 13, 2001

Printed in USA